Numerical study on the improvement of the cooling of a microprocessor by the use of nanofluids

TALOUB DJEDID[1], BOURAS ABDELKARIM[2], ZIED DRISS[3]
[1,2]Department of Physics, Faculty of Sciences, University Mohamed Boudiaf of M'sila, ALGERIA
[1]Laboratory of Materials Physics and its Applications, University Mohamed Boudiaf of M'sila, ALGERIA
[3]Department of Mecanics, Electromechanical Systems Laboratory, University of Sfax, TUNISIA

Abstract: - The numerical study on the improvement of the cooling of a microprocessor by the use of Nanofluids has been made. Natural convection is analyzed in a box fence with a temperature source encountered at its lower border and loaded with an Ethylene Glycol-Copper nanoparticle. This article explores the influences of relevant aspects such as thermal Rayleigh number, solid volume fraction, and enclosure dimensions on the thermal efficacy of the box fence, which are enhanced with an enlargement in thermal Rayleigh number and solid volume fraction. The results also illustrate that the change of the warmth transfer rate concerning the box dimensions of the enclosure is unlike at inferior and elevated thermal Rayleigh numbers. A simile is offered between the upshots got and the literature. Results were presented in terms of heat transfer rate depending on thermal Rayleigh number ($Ra_t = 10^3$, and 10^6), nanoparticle solid volume fraction ($0 \leq \varphi < 5\%$), and box dimensions. The results show that raising the solid volume fraction of the nanoparticles ($\varphi = 5\%$) drive a rise in the efficient conductivity of the working fluid and consequently the improvement of the heat transfer rate by approximately ≈ 10% per compared to the base fluid case.

Key-Words: - Natural convection, box enclosure, thermal Rayleigh numbers, nanofluid, volume fraction.

Received: June 23, 2021. Revised: January 14, 2022. Accepted: February 25, 2022. Published: March 26, 2022.

1 Introduction

In recent years, we continue to witness the unparalleled development undergone by power electronics, particularly in terms of miniaturization technology. However, this development is handicapped by the limitation of the cooling necessary to the evacuation of higher and higher heat fluxes from even smaller surfaces. The first generation of power electronics components were cooled by natural convection using air heaters. Then, and as this became insufficient, fans were integrated into it allowing air to be blown directly onto the fins constituting the radiator. Considerable investigations have been performed on the properties of nanofluids and their applications in warmth transfer systems. It is, thus, of basic interest to investigate innovative and functional techniques that support the natural convection outflow for different shapes of electronic constituents. The nanofluids have also been used to enhance the warmth transfer rate by increasing the thermal conductivities of the fundamental fluid using suspended nanoparticles. Among the works that exist, we quote some experimental and/or numerical works with/without the use of nanofluid.

Siddiqui et al. [1] performed an empirical investigation on flat warmth sink utilizing Al_2O_3 and CuO nanoparticles. Bahiraei et al. [2-4] optimized and investigated the efficiency and entropy generation of a combination nanofluid having graphene nanoplatelets adorned with silver nanoparticles in three separate liquid unions for CPU cooling. Hybrid nanofluids show a promising way to improve cooling in electronics. Sarafraz et al. [5] experimentally studied the thermic performance of a coolant bloc operating with gallium, a nanofluid (CuO/water), and clean water. The processor utilized in this investigation is rated at three conditions of standby, normal, and overload operating methods. The impacts presented that gallium is the considerable effective coolant between nanofluid and water in terms of convective thermic performance. Qi et al. [6-9] established and examined an empirical setting for the warmth transfer properties of CPU refrigerated by nanofluids. The impacts of nanoparticle mass particles and Reynolds numbers on warmth transfer and flow characteristics are discussed. It was also discovered that Al_2O_3-water and TiO_2-water nanofluids could decrease CPU temperature by 23.2% and 14.9% at most useful likened to water respectively. Sun et al. [10] experimentally measured in a liquid-cooled central processing unit (CPU) warmth sink the warmth transfer coefficient and the flow resistance coefficient of Cu-water and A12O3-water nanofluids. The results demonstrate that the cooling performance of a CPU warmth sink was remarkably improved by using the Cu-water and A12O3-water nanofluids and the exterior temperature of the CPU scrap was reduced by 4-18°C compared with demineralized water. Snoussi et al. [11] numerically treated the laminar flow of nanofluids in a 3D copper microchannel warmth sink (MCHS) with a rectangular enclosure and invariant warmth flux. The numerical consequences illustrate that the increase in warmth flux has a remarkably small influence on the warmth transfer coefficient for pure water, while an observable impact for the instance of a nanofluid. Shoukat et al. [12] investigated the stability of nanofluids and saw the warmth transfer improvement compared to water. Chen et al. [13] investigated numerically and experimentally cooling performance CPU, used TiO2-water 9% as coolant. The numerical results agree nicely with the empirical results. The results demonstrated that nanofluids can effectually decrease the middle CPU temperature by 4.54 ◦C at best compared to water underneath similar operational conditions. Izadi et al. [14] studied the thermal radiation and the thermogravitational transfer of a micropolar nano liquid in a permeable enclosure in the existence of the constant magnetic effect. Used the Galerkin finite element approach with the structured non-uniform gid is to estimate the developed equations. The main factors are Darcy–Rayleigh number, Darcy number, porosity, nanoparticle concentration, radiation parameter, vortex viscosity characteristic rand Hartmann number. The results demonstrate that the middle Nusselt number decreases with an increment of the Hartmann number for increased values of the thermal Rayleigh number, a small modification in the average Nusselt number can be located. Elbadawy et al. [15] numerically studied the effect of the use of nanofluids on the increase in warmth transfer and the aspects of fluid flow in a rectangular microchannel warmth sink. The results reveal that increasing the concentration of nanoparticles improves the cooling process. Amiri et al. [16] numerically studied in parallel micro-channels the design of micro-heat exchangers, the uniformities of flow and. Used Carboxy methylcellulose as a coolant. Studied the structures and effects of collectors on flow and temperature distributions. Maher et al. [17] developed, analyzed, and simulated a detailed, non-isothermal, three-dimensional computational fluid dynamics (CFD) model for fluid flow and heat transfer physiognomies. Nanofluids have been presented as efficient refrigerants to be used in this type of warmth sink to raise the rate of warmth dissipation. The results show that analyzing performance parameters as a function of Reynolds number is tricky and that utilizing nanofluids in a microchannel warmth sink is unusable because water is cheaper and safer. Mohd et al. [18] innovated to enhance warmth transfer performance in an MCHS to meet the cooling market of electronic devices established with high-power integrated circuit (microchip) boxes. The use of nanotechnology in the shape of a nanofluid in an MCHS has drawn the attention of investigators due to the dramatic improvement in thermal conductivity. The study showed that the combination MCHS delivers a more reasonable cooling performance than the MCHS with the single passive approach. Mokrane et al. [19] conducted numerical and empirical research to examine the elements of laminar flowing and compelled convection warmth transfer in micro-channels. Studied various cooling techniques to improve the warmth transfer methodology in electronic components. The results demonstrated that the micro warmth exchanger was competent to disperse about 70-78% of the warmth given off by the electronic element. Souby et al. [20] numerically evaluated the performance of the first and second laws of MCHS employing the novel cost-efficient binary/ternary combination nanofluids. The influences of hybrid nanofluid volume concentration and Reynolds number on the warmth transfer, pressure decrease combined thermal-hydraulic elements, and entropy generation elements of MCHS were examined. The results show that the $CuO/MgO/TiO_2$-water ternary combination nanofluid showed sounder warmth transfer efficacy than the MgO/TiO_2-water binary combination nanofluid. Ramadhan et al. [21] experimentally explored the stability of the tri-hybrid nanofluid for a volume concentration of 0.5 to 3.0% and temperature conditions of 30 to 70 °C to measure the thermal conductivity employing a heat analyzer. KD2 Pro thermal effects. The results illustrate that the tri-hybrid nanofluids with a concentration of 0.5% offered the lower sufficient thermal conductivity of 13.4% at 70°C. Payal et al. [22] presented detailed research of nanotechnology, its process to nanoelectronics, classing and kinds of nanomaterials employed in nanoelectronics, application regions of nanoelectronics, and calculating instruments with nanoscale characterization. Sanpui et al. [23] investigated the use of a Cu-water nanofluid numerically for the simulation of warmth transfer performance due to transient laminar natural convection inside a square enclosure with a protruding isothermal heating element. Mirzaei et al. [24] studied the flowing and warmth transfer of a second-order viscoelastic fluid in an axisymmetric porous-walled canal for turbine cooling applications are investigated. Çakmak et al. [25] numerically investigated the improvement of warmth transfer in an enclosure using the nanofluid Al_2O_3-EG. Revealed the effects generated by delays in the viscosity and thermal conductivity of the nanofluid on the laminar natural convection warmth transfer happening in a square fence. Discovered that nanofluid viscosity was the considerable effective aspect for warmth transfer rate. Abdulkadhim et al. [26] numerically used natural convection in complicated fence shapes such as trapezoidal, parallelogrammic, elliptic, and wavy geometries, considering different approaches. Examined the effect of the position of the inside of the body and its size. Roy et al. [27] numerically investigated the electrohydrodynamic enhancement of the laminar flow of nanofluids with natural convection in a shut cavity. The consequences show that the electric field induced by the charged particles significantly influences the flow field inside the cavity.Taloub et al. [28, 29] numerically investigated natural convection of steady-state laminar heat transfer in a ring between two hexagonal cylinders and a horizontal ring within a heated inner elliptical surface and a cold outer square surface. A Cu-water nanofluid passes through this annular space. Studied the impacts of various thermal Rayleigh numbers, nanoparticle volume fraction, and the effect of inner cylinder eccentricity on natural convection. Aminossadati et al. [30] examined the influences of relevant parameters such as thermal Rayleigh number, solid volume fraction, warmth source place, and fence vertex angle on thermal implementation in an isosceles triangular fence with warmth source found at its lower wall and refilled with an Ethylene Glycol-Copper nanofluid. These effects show that the variation of the heat transfer rate for the enclosure apex angle and the placement and measurements of the warmth source is various at inferior and increased thermal Rayleigh numbers. Haq et al. [31] presented a study on the thermal management of water-based single-walled carbon nanotubes (SWCNTs) interior the partially warmed triangular cavity with a warmed cylindrical block. The thermal conductivity of the liquid is completely enhanced by presenting the SWCNT and detailed conditions are presented at the internal circular cylinder. The numerical resolution is desired utilizing the finite element approach (FEM). Simulation is affected by the effects of cylindrical blocks, heated lengths, Rayleigh number, the volume fraction of nanoparticles, and magnetic parameters on warmth transfer rate, flowing speed areas, and temperature diffusion. The analysis concludes that at the hectic length, the warmth transfer rate for the warm cylinder is lower than that for the cool cylinder. Sojoudi et al. [32] realized a mathematical model to simulate the mixed convection of the Al_2O_3-water nanofluid in a triangular space driven per the lid utilizing the Lattice Boltzmann approach (LBM). Different thermal conductivities and viscosities of the working nanofluid were taken into account. For different Richardson numbers, aspect ratios, solid volume fractions of nanoparticles, and different frequencies and amplitudes of wall cover sinusoidal thermal forcing. The grid sensitivity test was performed and the results were validated against the experimental study. Thangavelu et al. [33] numerically investigated the warmth transfer per natural convection interior a fence with central heating employing a nanofluid. The effect of different central heater lengths on the flowing and temperature domains is analyzed for various thermal Rayleigh numbers. The numerical results illustrate that the warmth transfer raises with the increase in the length of the heating element at the perpendicular and horizontal positions for rising values of the thermal Rayleigh numbers. In certain, a more heightened accumulation in warmth transfer is received with a heater found in a perpendicular place of maximum height. Oudina [34] numerically studied the hydrodynamic and thermic aspects of Titania nanofluids loading a cylindrical ring. Ethylene glycol, motor oil, and water are utilized as basic fluids. Maxwell's prototype for warmth transfer in nanofluids is observed to count for the impacts of nanoparticle volume particle diffusion on the various equations, in that a formed computer code is utilized established on the finite volume approach associated with the SIMPLER algorithm. The impacts of different parameters on the local Nusselt number are examined. Loenko et al. [35] dedicated the mathematical modeling of the term gravitational convection of a non-Newtonian fluid in a shut enclosure cavity with a local source of inner volumetric warmth generation. The Ostwald-de Waele power-law model describes the behavior of the fluid. The influences of thermal Rayleigh number, power-law index, and thermal conductivity ratio on warmth transfer and flowing form are reviewed. Dogonchi et al. [36] numerically studied the part of natural convection and thermic radiation on the thermo-hydrodynamics of warmth transfer of nanofluids in a ring between a corrugated circular cylinder and a diamond-shaped fence subjected to an invariant magnetic field. The effects of maintaining physical parameters, thermal Rayleigh number, radiation parameter, Hartmann number, factor ratio, the form aspect of nanoparticles, and solid volume particle of nanoparticles on the thermo-hydrodynamics of the flowing are reviewed. It evolves evident that the local warmth transfer rate lowers with increasing aspect ratio in the non-attendance of Hartmann number. Oudina et al. [37] numerically analyzed the effects of the place of a thermic source on the floating convection of nanofluids in an annular area. Five different positions of thermal sources alongside the internal cylinder of the annular space were studied. The main purpose is to determine the optimal placement of the source to maximize or minimize the thermic transportation at various values of thermal Rayleigh number and various volume particles of the nanoparticle. The place of the heat source has a deep effect on the flowing and temperature patterns as agreeably as the heat transfer of the discreet source to the nanofluid. Laidoudi et al. [38] investigated numerically two-dimensional buoyancy-driven flowing in a shut annular area. The studied field includes a pair of circular cylinders of identical size arranged in a team enclosed in a circular loaded with incompressible Newtonian fluid. The influences of the thermic buoyancy force, the thermophysical aspects of the fluid, the length of the internal cylinders on the flowing patterns interior the circular field, and the rate of warmth transfer exchanged between the internal cylinders and the flowing of the fluid have been studied. The results showed that the studied guiding parameters affect significantly. An addition in the diameter of the internal cylinders creates the influence of buoyancy force on fluid flowing and warmth transfer insignificant for any values of thermophysical parameters. Nguyen et al. [39] simulated the thermic conduct in a curved porous field is examined in the formation of an ethylene glycol-founded nanofluid. The term radiative source was presented and nanoparticles of various forms namely: Platelets, bricks, cylindrical and spherical are distributed within the basis fluid. The effects of permeability, voltage, radiation parameters, and nanoparticle form on streamlines, isotherms, Nusselt number have been indicated. Ranges of specified parameters are included, which are: the voltages the Darcy number the shape of the nanoparticles, and the radiative factor. The results showed that the convection increases with the height of Da. The convective flowing evolves more powerful due to the addition of higher voltage. Umavathi et al. [40] studied double-diffusive convection in a saturated horizontal permeable coating of a saturated incompressible torque stress nanofluid with thermal conductivity and viscosity depending on the volume fraction of the nanoparticles. Nonlinear theory based on the Fourier series approach representation is used to capture the conduct of warmth and mass transfer. The torque constraint parameter is found to improve the stability of the approach in the stationary and oscillatory convection modes. Viscosity proportion and conductivity proportion both improve warmth and mass transfer. The transitory Nusselt number turns out to be oscillatory when the time is little. However, when time evolves extremely considerably, any three values of the transitory Nusselt number come to their steady-state values. Lakshmi et al. [41] analytically studied natural convection in cylindrical permeable rings flooded by a nano liquid whose internal and external perpendicular radial fences are respectively subjected to invariant fluxes of warmth and mass utilizing the changed Buongiorno-Darcy model (MBDM) and Oseen's linearization method. The thermophysical properties of a permeable medium flooded with nano liquid are sported employing phenomenological rules and mix hypothesis. The influence of different parameters and the particular impacts of five various forms of copper nanoparticles on speed, temperature, and warmth transportation is located. From the investigation, it is evident that the accumulation of a dilute concentration of nanoparticles raises the sufficient thermic conductivity of the technique and thus rises the speed and warmth transportation, and reduces the temperature. The highest warmth transport is performed in a superficial cylindrical ring analogized to square and long circular rings. Increasing the radius of the internal solid cylinder aims to reduce warmth transport. Mehryan et al. [42] numerically studied the natural convection of Ag-MgO/water nanofluids in a permeable fence utilizing a local thermic non-equilibrium model. Darcy's model is used. The key parameters of this analysis are the thermal Rayleigh number, the porosity, the volume particle of the nanoparticles, the interface convective warmth transfer coefficient, and the thermic conductivity proportion of two permeable phases. It is demonstrated that the dispersion of Ag-MgO hybrid nanoparticles in water extremely reduces the heat transportation through two phases of the porous enclosure. Abdulkadhim et al. [43] summarized previous studies relating to heat flow in enclosures of different square, rectangular and triangular enclosure geometries. Enclosures filled with different fluids such as traditional fluids and nanofluids, Newtonian and non-Newtonian fluids, and multilayer techniques. Different numerical models have been reworded. The effect of diverse parameters such as Rayleigh, Darcy, Bejan, and Hartmann numbers, the charging of nanofluids, various thermic cases of the devoted border conditions, the angle of tilt, the number of undulations, the presence of 'an internal body, and considerable other parameters affecting and hardly impacting entropy generation and warmth transfer has been defined. Alomar et al. [44, 45] suggested a numerical investigation on natural convection in a non-Darcy permeable layer surrounded by two horizontal areas including sinusoidal temperature shapes with phase and wavenumber variance. Simulations have been executed for wide fields of coefficient of inactivity, thermal conductivity ratio, phase shift, modified Rayleigh number, wavelength, and dimensionless heat transfer coefficient. A considerable improvement of the fluid, solid and global Nusselt numbers were marked with a decrease in Fs/Pr* and β and an increase in k, K r, and H. The influence of H on the non-equilibrium zone is more obvious than Kr. Ali et al. [46] numerically studied the mixed convection caused by two aligned horizontal agitated cylinders implanted in a square fence with symmetrical spaces on the inferior and superior surfaces of the fence. The parameters were protected a broad field of gap size between two cylinders, opening vent, Reynolds number, and Richardson number, while Prandtl number remained fixed. The numerical effects show that the mean of the hectic cylinders raised with the increase of Ri, Re, and the beginning of the vent. The optimal improvement was found when the gap size was under the full aperture size case.

Nowadays, air-cooling has also become insufficient and more and more people are moving towards nanofluid cooling. In this context, we conducted a numerical study on the cooling of a heating system simulating a microprocessor like those that equip PCs. We used nanofluid cooling in a box in order to show the cooling efficiency on the one hand and to determine the parameters that can affect it on the other hand. To protect microprocessors at high frequencies against excessive heating, the use of another cooling system is essential. We then proposed to carry out a numerical study on a prototype of a nanofluid box in order to evacuate the heat emanating from a thermal source simulating a microprocessor.

2 Problem modeling and resolution

First, we present the geometry and the system of equations that governs the flow and the transfer of heat by convection with the use of nanoparticles. Then, we will present how the resolution of our two-dimensional problem is implemented by the fluent software.

2.1 Geometry and problem formulation

The current model consists of a box enclosure loaded with an Ethylene Glycol–Copper nanofluid (figure. 1). A warmth fount of rib w and relatively elevated temperature (T_h) is found at the level of the heat-insulated lower border. whilst the borders of the box of the fence are retained at a somewhat more inferior temperature (T_c). The thermal Rayleigh's number, Rat, ranges from 10^3 to 10^6. The flow is considered to be two-dimensional, the flow is convection natural laminar of nanofluid Ethylene Glycol–Copper (EG–Cu). The nanofluid is assumed incompressible and Newtonian by negligible viscous diffusion and pressure working. The thermophysical properties of the nanofluid are supposed constant except for the density, which changes according to the Boussinesq approach. The Boussinesq approximation is used to model the buoyancy effect. The acceleration due to gravity acts in the negative y-direction.

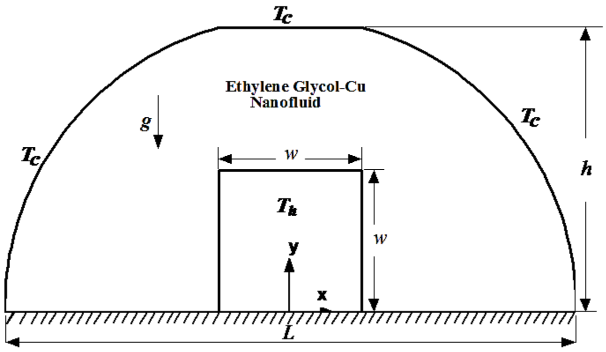

Fig. 1 Schematic graph of the physical prototype

The dimensionless equations governing the laminar flow of our problem below the non-dimensional variables are written as follows [47-51]:

$$X=\frac{x}{L}, Y=\frac{y}{L}, U=\frac{uL}{\alpha_f}, V=\frac{vL}{\alpha_f}, \theta=\frac{T-T_c}{T_h-T_c}$$

$$P=\frac{\bar{p}L^2}{\rho_{nf}\alpha_f^2}, Pr=\frac{\vartheta_f}{\alpha_f}, Ra_t=\frac{g\,\beta_f\,(T_h-T_c)\,L^3}{\alpha_f\,\vartheta_f} \tag{1}$$

Continuity equation

$$\frac{\partial U}{\partial X}+\frac{\partial V}{\partial Y}=0 \tag{2}$$

Momentum equations

$$U\frac{\partial U}{\partial X}+V\frac{\partial U}{\partial Y}=-\frac{\partial P}{\partial X}+\frac{\mu_{\mathrm{nf}}}{\rho_{\mathrm{nf}}\,\alpha_f}\left(\frac{\partial^2 U}{\partial X^2}+\frac{\partial^2 U}{\partial Y^2}\right) \tag{3}$$

$$U\frac{\partial V}{\partial X}+V\frac{\partial V}{\partial Y}=-\frac{\partial P}{\partial Y}+\frac{\mu_{\mathrm{nf}}}{\rho_{\mathrm{nf}}\,\alpha_f}\left(\frac{\partial^2 V}{\partial X^2}+\frac{\partial^2 V}{\partial Y^2}\right)+\frac{(\rho\,\beta)_{\mathrm{nf}}}{\rho_{\mathrm{nf}}\,\beta_f}Ra_t\,Pr\,\theta \tag{4}$$

Energy equations

$$U\frac{\partial \theta}{\partial X}+V\frac{\partial \theta}{\partial Y}=\frac{\alpha_{\mathrm{nf}}}{\alpha_f}\left(\frac{\partial^2 \theta}{\partial X^2}+\frac{\partial^2 \theta}{\partial Y^2}\right) \tag{5}$$

Where: U and V are the dimensionless speeds in the X and Y directions, respectively. The physical characteristics of Ethylene Glycol and nanoparticles are presented in Table 1.

Table 1 Physical characteristics of Ethylene Glycol and Cu [52, 53]

	$\rho(\frac{Kg}{m^3})$	$C_p\,(\frac{J}{kg.K})$	$K\,(\frac{W}{m.K})$	$\beta\,(\frac{1}{K})$	$\mu\,(Ps.s)$
E-G	1109	2400	0.26	6.5x10^{-4}	0.02
Cu	8933	385	401	1.67x10^{-5}	-

The effective nanofluid density (ρ_{nf}) is given by [54]:

$$(\rho)_{\mathrm{nf}} = \phi\,\rho_p + (1-\phi)\rho_f \tag{6}$$

The effective dynamic viscosity of nanofluid (μ_{nf}) is presented by [54]:

$$(\mu)_{nf} = \frac{\mu_f}{(1-\phi)^{2.5}} \tag{7}$$

The heat capacity of nanofluid is given by [54]:

$$\left(\rho C_p\right)_{\mathrm{nf}} = \phi\left(\rho C_p\right)_p + (1-\phi)\left(\rho C_p\right)_f \tag{8}$$

The thermic expansion coefficient of the nanofluid is defined through:

$$(\rho\,\beta)_{nf} = \phi\,(\rho\,\beta)_p + (1-\phi)(\rho\,\beta)_f \tag{9}$$

The effective thermal conductivity of the EG–Cu nanofluid for spheroidal nanoparticles is [55]:

$$K_{nf} = K_f\,\frac{(K_p+2K_f)-2\phi(K_f-K_p)}{(K_p+2K_f)+\phi(K_f-K_p)} \tag{10}$$

These various boundary conditions in dimensional format can be summarized as:
The initial conditions are:

$$U = V = 0 \tag{11}$$

$$\theta(X,Y) = 0 \tag{12}$$

Moreover, the boundary limitations concerning the problem are:
Along the sides of the enclosure (box):

$$U = V = 0 \tag{13}$$

$$\theta(X,Y) = 0 \tag{14}$$

Along the sides of the lower wall (CPU):

$$U = V = 0 \tag{15}$$

$$\theta(X,Y) = 1 \tag{16}$$

Alongside the horizontal side of the fence:

$$\frac{\partial\theta}{\partial Y} = 0 \tag{17}$$

2.2 Numerical method

The equations are treated consecutively by utilizing the isolated method. The use of fluent software allows us to build a numerical model capable of dealing with the problem of flowing and warmth transfer by convection with the use of nanoparticles for the two-dimensional case. First, it is necessary to generate the mesh using Gambit software (see figure 2).This approach has the advantage of meeting the mass, the conservation of the momentum, and the energy in all the considered volumes as well as in all the fields of calculation with the assessed boundary conditions is founded on the finite volume approach. To confirm a satisfactory solution in regions with a high-temperature gradient, livery structured mesh close was supposed. The second-order scheme was thought since it allows some stability and minimizes the numerical diffusion though it can make the calculation diverge. The simple algorithm of Patankar and Spalding [56] was employed for speed-pressure coupling. In addition, the computational residue was utilized to confirm the convergence and the stability of the resolution.
Another helpful quantity like the Nusselt number for every flank from the hot walls is perhaps chosen afterward resolving the dominant equations from U, V, and θ. The local Nusselt numbers from the right side, left side, and topside from the hot walls represented as [30]:

$$Nu_R = -\frac{k_{nf}}{k_f}\frac{\partial\theta}{\partial X}\bigg|_{\text{Right side}} \tag{18}$$

$$Nu_L = +\frac{k_{nf}}{k_f}\frac{\partial\theta}{\partial X}\bigg|_{\text{Left side}} \tag{19}$$

$$Nu_T = -\frac{k_{nf}}{k_f}\frac{\partial\theta}{\partial Y}\bigg|_{\text{Top side}} \tag{20}$$

Therefore, the mean Nusselt number from every flank from the hot wall is defined per incorporating the local Nusselt number alongside the area of the individual side from the hot walls [30]:

$$Nu_{avg,R} = \frac{1}{W}\int_0^W Nu_R.\,dY \tag{21}$$

$$Nu_{avg,L} = \frac{1}{W}\int_0^W Nu_L.\,dY \tag{22}$$

$$Nu_{avg,T} = \frac{1}{W}\int_{-\frac{W}{2}}^{+\frac{W}{2}} Nu_T.\,dX \tag{23}$$

The total mean Nusselt numbers for the hot wall perhaps received by incorporating the local Nusselt numbers alongside the right, left, and top sides from the hot walls.

$$Nu_{avg,hot\ wall} = \frac{1}{3W}\left[+\int_0^W Nu_L.\,dY + \int_{-\frac{W}{2}}^{+\frac{W}{2}} Nu_T.\,dX + \int_0^W Nu_R.\,dY\right] \tag{24}$$

The evolution of the mean Nusselt number for five various grille dimensions is analyzed to examine the freedom from the resolution with the grille dimension. Three various outer wall heights of 0.5, 0. 4375, and 0.375 are evaluated, and the performance for φ = 0.05, W=0.25, and $Ra_t = 10^5$ are shown in fig. 2. A mesh dimension of 100 × 100 meets the needs of the investigation of network freedom and

calculation time boundaries. The convergence measure to lower the greatest residual mass from the grille command volume below 10^{-12}.
To give credibility to our current numerical study with the presence of nanoparticles, the numerical model was validated with the work of Aminossadati et al. [30] who numerically studied two-dimensional laminar natural convection into an isosceles triangular fence with the use from nanofluids are presented in fig. 3.

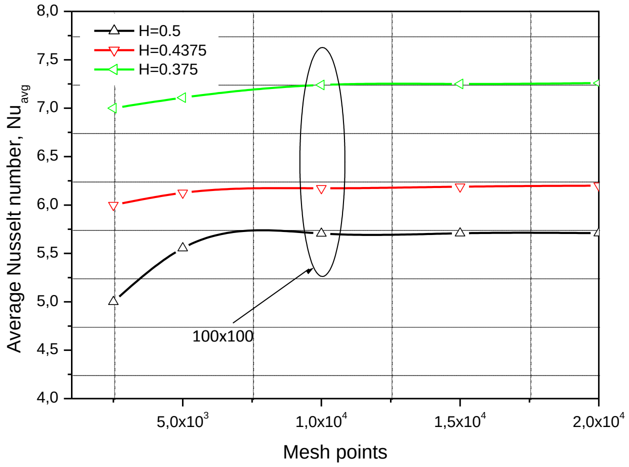

Fig. 2 Mesh independence analysis

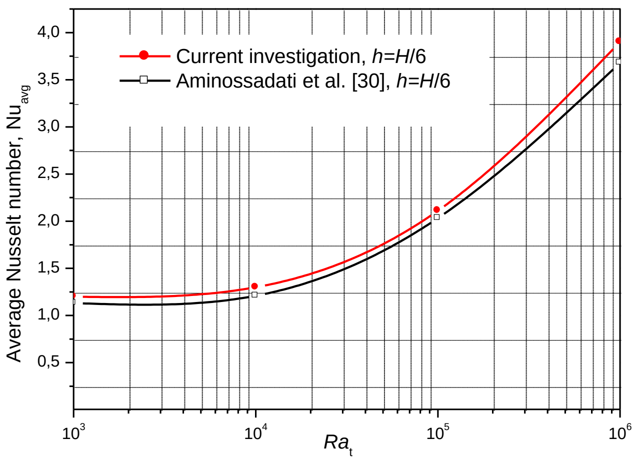

Fig. 3. Comparison of the current investigation versus Aminossadati et al. [30].

3. Results and commentary

In the current investigation, the solid volume fragment ($0 \leq \varphi \leq 0.05$), the thermal Rayleigh number is supposed to be in the following ranges ($10^3 \leq Ra_t \leq 10^6$), the height of the box ($0.3125 \leq H \leq 0.5$), and the length of each side of the hot wall is fixed at (W=0. 25). The influences of each of cited parameters are analyzed individually in various sections.
The effect of the adding from copper nanoparticles in the basis fluid about the streamlines and the isotherms from diverse thermal Rayleigh numbers $Ra_t=10^4$, 10^5, and 10^6 illustrated in figure 4, which highlights in first the effect of the increase in the thermal Rayleigh number about the flow from the nanofluid (φ=0.05) and sheer ethylene glycol (φ=0). From streamlines, there are considerable dissimilarities in the central area, specifically when the thermal Rayleigh number is large ($Ra_t \geq 10^5$). The addition of nanoparticles increases the intensity of the streamlines, particularly within the central area. Contrary, when the thermal Rayleigh number is smaller, the weakening of the intensity from the flow is noticed compared to the flow of the base fluid. Nevertheless, nearby isothermal walls, the dissimilarity into the greatness from the current function is much little. From isotherms, moderately large dissimilarities are followed into the central area and near the lid and lowest walls whenever the thermal Rayleigh number is large The temperature gradient around the isothermal walls from the nanofluid is lightly more considerable than that from pure ethylene glycol, although the difference increases with increasing thermal Rayleigh number, demonstrating that greater warmth transfer, happens when the operating fluid is a nanofluid. For every, the thermic Rayleigh number values, the contours of the streamlines and isotherms are symmetrical concerning the perpendicular median of the box. Increasing Rayleigh number intensifies convection, buoyancy forces become stronger: the upper nodes get stronger and then start to merge with the lower ones due to the prevailing convective heat transfer mode as shown in figure 4. At $Ra_t=10^6$, figure 4 shows that the isothermal lines change and ultimately adopt the form of a mushroom either for the nanofluid or the pure EG. The temperature diffusion is lowering from the warm wall to the cold wall. The directorate of deformity of the isotherms conforms to the directorate of rotation of the streamlines. In the laminar regime, it can be said that, underneath the movement of the action of the particles which take off for the warm wall at the level of the axis of symmetry, the isothermal lines “vault” and move far from the wall at this point. The worths from the current functions for the nanofluid and the pure fluid increase which means that the convection intensifies. Comparison between nanofluid and pure fluid shows that at heightened thermal Rayleigh number, circulating cells from nanofluid are more powerful than those from pure fluid, unlike at inferior thermal Rayleigh number.

DOI: 10.37394/232012.2022.17.8

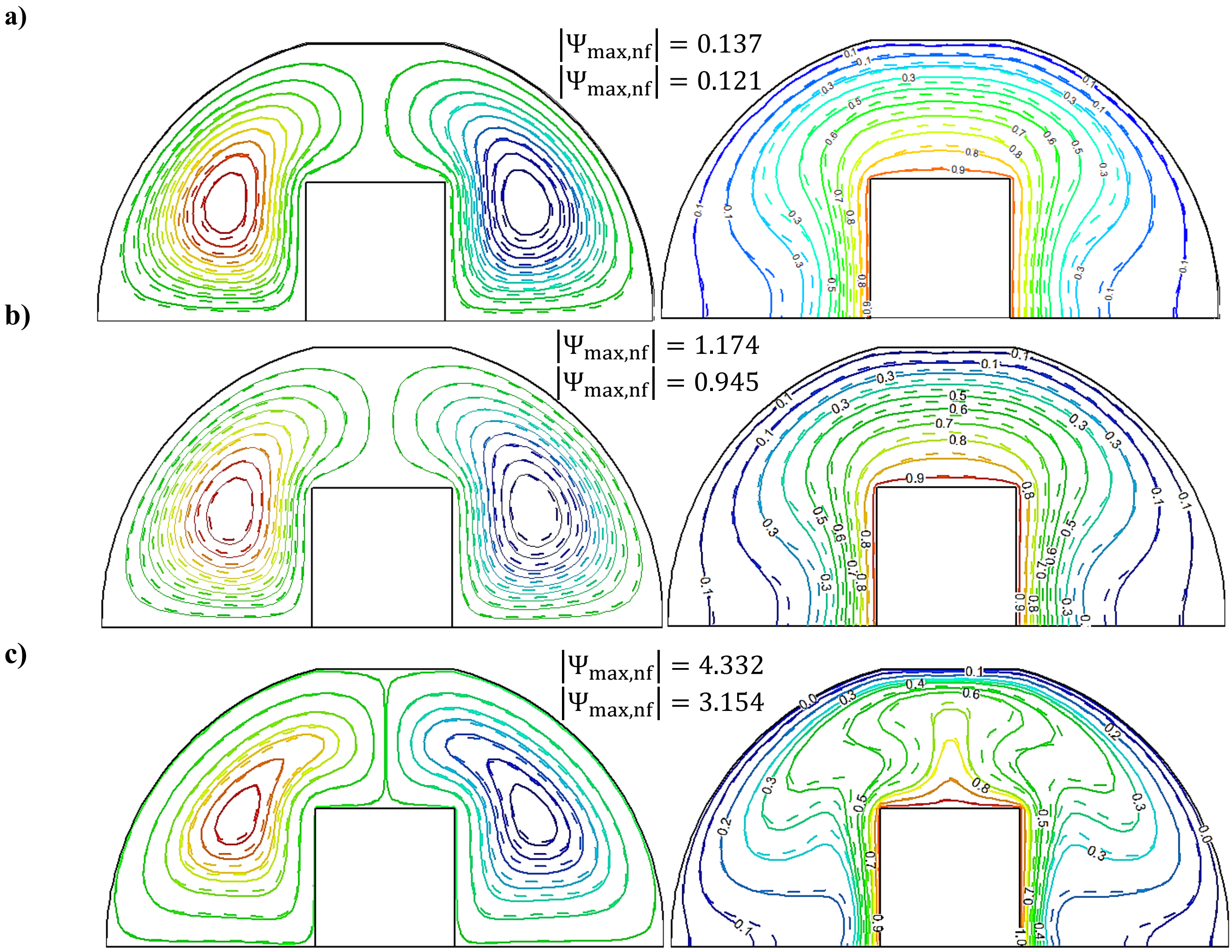

Fig. 4. Isocurrents (left) and isotherms (right) from H=0.5, W=0.25, nanofluid with φ = 0.05 (____) and pure fluid (− − −), (a) Ra_t=10[4], (b) Ra_t=10[5], (c) Ra_t=10[6]

Figures 5a and 5b show the evolutions of the dimensionless temperature (θ) and the perpendicular component of the velocity (V) of the flow, on the horizontal direction expanding on the upper flank from the hot wall (Y = 0.1), respectively. These figures make it possible to confirm the results obtained previously and to understand the flow behavior inside the box for the pure EG and the nanofluid EG-Cu at various thermal Rayleigh numerals. The evolutions of the dimensionless temperature alongside the axis Y=0.1 increase for the leftside of the box towards the side of the hot wall. Along this axis, as the thermal Rayleigh number raises the temperature lowers. At $Ra_t=10^6$, the EG–Cu nanofluid exhibits more increased velocity and more inferior temperature likened to pure fluid owing to more powerful buoyant fluxes in increased thermal Rayleigh numerals. The increase in the magnitude of V with increasing thermal Rayleigh number is a motion of more powerful floating fluxes in the increased thermal Rayleigh number box. This explains why heat transfer is in the convection mode at high thermal Rayleigh number, while conduction is accountable for warmth transfer in inferior thermal Rayleigh number.

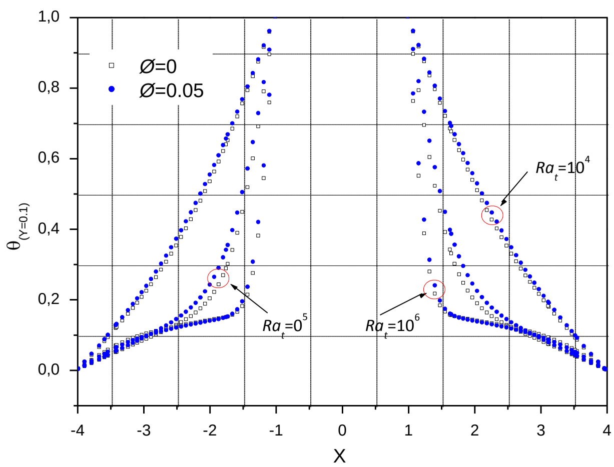

Fig. 5a Temperature form in Y = 0.1 from both pure fluid and nanofluid (H =0.5, W=0.25)

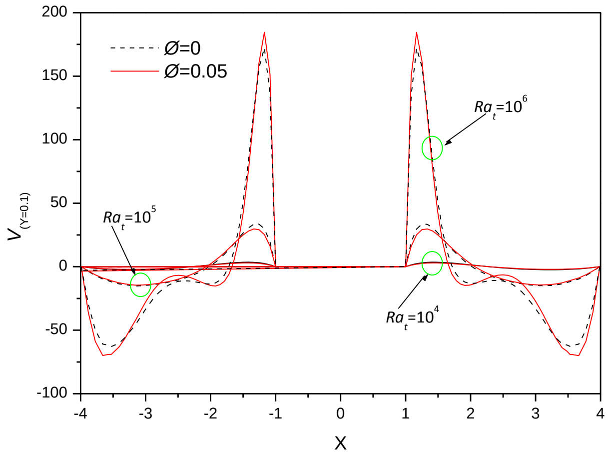

Fig. 5b Perpendicular velocity form in Y = 0.1 from both pure Fluid and Nanofluid (H =0.5, W=0.25)

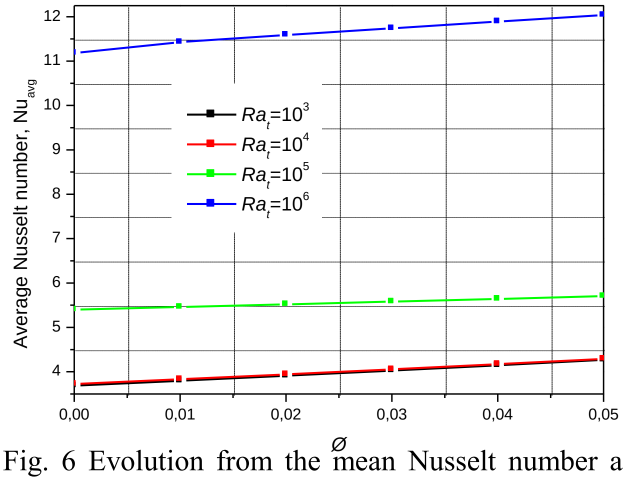

Fig. 6 Evolution from the mean Nusselt number a fonction φ with various Ra_t (H =0.5, W=0.25)

The profile of the mean Nusselt number as a function from the solid volume fraction is shown in figure 6. We notice that the increase in inertial forces promotes the warmth transfer process. Also, raising the solid volume fraction of the nanoparticles improves the heat transfer rate. This expansion is owing to the improvement in the sufficient thermic conductivity of the nanofluid as the volume of nanoparticles rises.

In figure 7, the influence of the box height (H) upon the warmth transfer performance from the processor cover box is examined. We consider that W = 0.25 and φ = 0.05. This figure illustrates the isocurrents and isotherms for $Ra_t = 10^5$ and three various heights (H = 0.3125, 0.375, and 0.4375).

The effects demonstrate that for all heights, two cells are symmetric that is to say; the minimal and maximal valors to the isocurrents of the two cells are the same, and circulating counter-rotating inside the box. When the values of the sides of the bottom wall are fixed, as the height decreases, the box becomes less, and the circulating cells evolve better defined. Therefore, a decrease into height leads to a diminution into the force from the rolling cells, not to say that the rate of warmth transfer will be decreased from high heights. When the top side from the warmth source approaches the cold top wall and the rate of conductive heat transfer should increase.

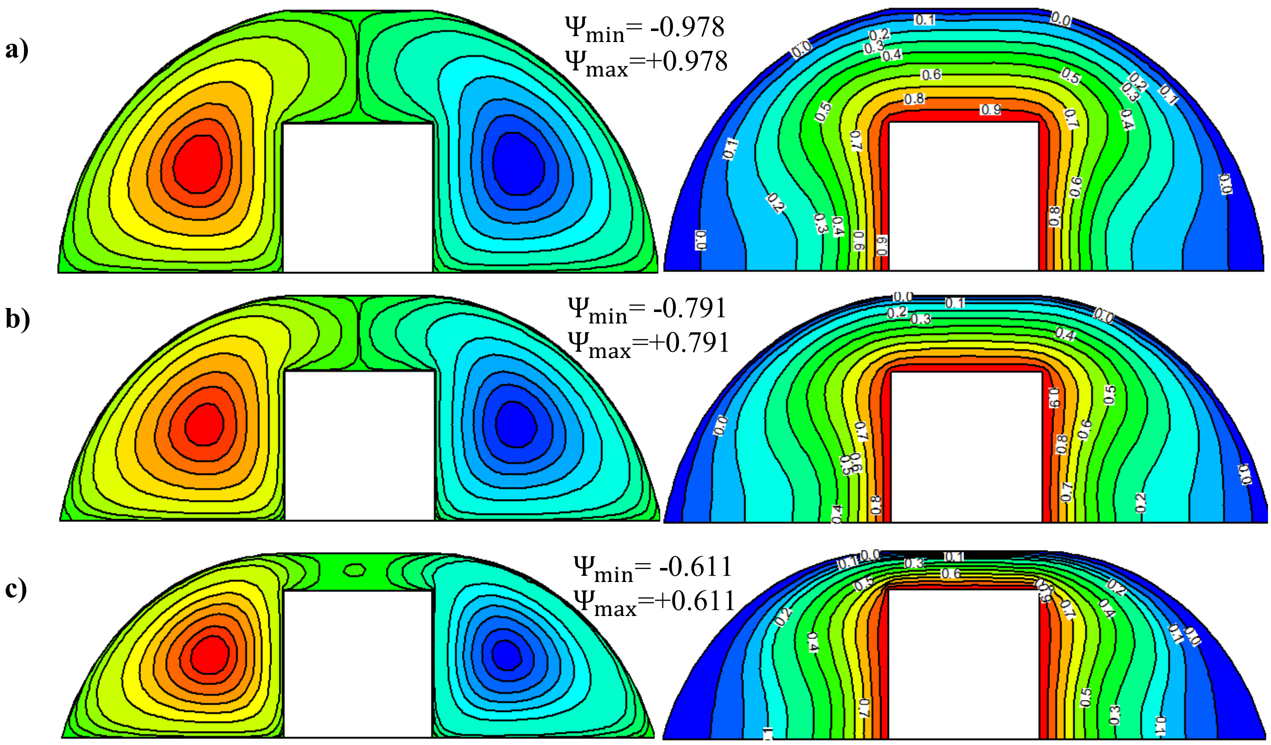

Fig. 7. Streamline (left) and isotherms (right) for $Ra_t = 10^5$, φ = 0.05, W = 0.25, (a) H = 0.4375, (b) H = 0.375, (c) H = 0.3125.

Figure 8 presents the development of the mean Nusselt number as a function from the height (H) of the upper wall for various thermal Rayleigh numbers. At considerable values of the height H, a large distance exists between the three sides of the hot wall and the cold walls of the box. Therefore, as the thermal Rayleigh number raises, the buoyancy strengths and the convective flowing domain evolve more powerful. Unlike small values of the height, the space evolves less, determining the force of the convective flowing area.
It is noted in this figure that for all valor of the thermic Rayleigh number save from $Ra_t = 10^6$, the mean Nusselt number of the hot wall lowers as the warmth source displaces far from the cool wall. This is due to the decrease of warmth transfer by conduction. At $Ra_t = 10^6$, as height raise, the mean Nusselt number first lowers and yet rises owing to the reinforcement of floatable flows [30].

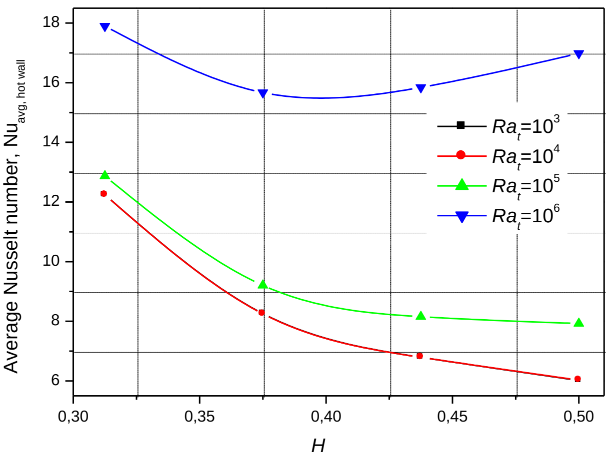

Fig. 8. Evolution of mean Nusselt number from hot wall with H at different Ra_t (φ = 0.05, W =0.25).

Figure 9 illustrates the interpretation of the ratio of the average Nusselt number of the nanofluid to the average Nusselt number of the pure fluid ($Nu_{\mathrm{avg,nf}}/Nu_{\mathrm{avg,f}}$) with the volume fraction φ at different thermal Rayleigh numerals.
The evolutions show that an increase in the volume fraction conducts to raise in the $Nu_{\mathrm{avg,nf}}/Nu_{\mathrm{avg,f}}$ for all the thermal Rayleigh numbers supposed. The rate of this augmentation is considerably observable in the results received.

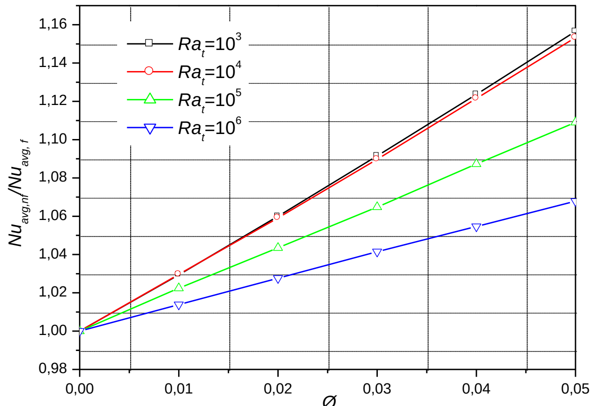

Fig. 9 Variation of $Nu_{\mathrm{avg,nf}}/Nu_{\mathrm{avg,f}}$ with φ at different thermal Rayleigh number

4 Conclusion

A two-dimensional numerical investigation on the improvement from the cooling of a CPU by the use of nanofluids. The fluent software was used to create the geometry and define the digital model of our problem. The effects of thermal Rayleigh number ($10^3 \le Ra_t \le 10^6$), nanoparticle solid volume fraction ($0 \le \varphi \le 5\%$), and top box height were investigated numerically on flux, temperature fields, and the rate of warmth transfer.
The main results are presented below:
* The utilization of nanoparticles in the basis fluid increases the thermic conductivity of the fluid and thus increases the warmth transfer.
* Thermal conduction within the fluid and between the fluid and the nanoparticles appears to be the dominant factor in this enhancement. It can be noticed that these significant improvements. In particular, we observed that the efficacious thermic conductivity of this nanofluid increases with the concentration from nanoparticles.
* For $Ra_t = 10^6$ and H=0.5, the results show that the increase into the solid volume fraction from the nanoparticles (φ = 5%) conducts to an expansion in the effective conductivity of the working fluid and consequently the increase in transfer rate. the heat of about ≈ 10% likened to the basis fluid instance. At lower thermal Rayleigh numbers, the warmth transfer rate rises always with the height of the enclosure (box).
* The growth in the thermal Rayleigh number amplifies the speed and temperature areas, thus inducing a transition from a conduction mode to a convection mode.
* The temperature and the flux fields are symmetrical for all lengthiness. The most increased warmth transfer rates are received from the inferior height. Yet, from lengthier heights, the warmth transfer rate initial lowers and then rises as the height raise

Nomenclature		*Greek symbols*	
C_p	Specific heat, $Jkg^{-1}K^{-1}$	α	Thermal diffusivity, m^2s^{-1}
g	Gravitational acceleration, ms^{-2}	β	Thermal expansion coefficient, K^{-1}
h	Height of enclosure upper wall, m	φ	Solid volume fraction
H	Dimensionless cold wall height (h/L	μ	Dynamic viscosity, $N.s.m^{-2}$
k	Thermal conductivity, $Wm^{-1}K^{-1}$	ν	Kinematic viscosity, m^2s^{-1}
L	Length of enclosure bottom wall, m	θ	Dimensionless temperature ($(T-T_c)/(T_h-T_c)$)
Nu	Local Nusselt number	ρ	Density, kg/m^3
Nu_{avg}	Average Nusselt number	ψ	Stream function
p	Fluid pressure, Pa		
P	Dimensionless pressure ($\bar{p}L^2/\rho_{nf}\alpha_f^2$)	*Subscripts*	
Ra_t	Thermal Rayleigh number ($g\beta_f(T_h-T_c)L^3/\alpha_f\vartheta_f$)	c	Cold wall
T	Temperature, K	f	Fluid (pure)
u, v	Velocity components in x, y directions, $m\ s^{-1}$	h	Heat source
U, V	Dimensionless velocity components ($u\,L/\alpha_f, v\,L/\alpha_f$)	L	Left side
w	Heated wall length, m	nf	Nanofluid
W	Dimensionless heated wall length (w/L)	R	Right side
x, y	Cartesian coordinates, m	T	Top side
X, Y	Dimensionless coordinates (x/L, y/L)		

References

[1] Siddiqui, A. M, Nasir, A, and Arsha, W, Evaluation of Nanofluids Performance for Simulated Microprocessor, *Thermal Science*, Vol.21, No.5, 2017, pp. 2227-2236.

[2] Bahiraei, M, and Heshmatian, S, Efficacy of a novel liquid block working with a nanofluid containing graphene nanoplatelets decorated with silver nanoparticles compared with conventional CPU coolers, *Appl. Therm. Eng*, Vol.127, 2017, pp. 1233-1245.

[3] Bahiraei, M, and Heshmatian, S, Optimizing energy efficiency of a specific liquid block operated with nanofluids for utilization in electronics cooling a decision-making based approach, E*nergy Convers. Manag*, Vol. 154, 2017, pp. 180-190.

[4] Bahiraei, M., and Heshmatian, S, Application of a novel biological nanofluid in a liquid block heat sink for cooling of an electronic processor: thermal performance and irreversibility considerations, *Energy Convers. Manag,* Vol. 149, 2017, pp. 155-167.

[5] Sarafraz, M.M., Arya, A., Hormozi, F., and Nikkhah, V, On the convective thermal performance of a CPU cooler working with liquid gallium and CuO/water nanofluid: a comparative study, *Appl. Therm. Eng*, Vol. 112, 2017, pp. 1373-1381.

[6] Qi, C., Hu, J., Liu, M., Guo, L., and Rao, Z, Experimental study on thermo-hydraulic performances of CPU cooled by nanofluids, *Energy Convers. Manag*, Vol. 153, 2017, pp. 557-565.

[7] Qi, C., Zhao, N., Cui, X., Chen, T., and Hu, J, Effects of half spherical bulges on heat transfer characteristics of CPU cooled by TiO_2-water nanofluids, I*nt. J. Heat Mass Tran*, Vol.123, 2018, pp. 320-330.

[8] Zhao, N., Qi, C., Chen, T., Tang, J., and Cui, X, Experimental study on influences of cylindrical grooves on thermal efficiency, exergy efficiency and entropy generation of CPU cooled by nanofluids, *Int. J. Heat Mass Tran*, Vol. 135, 2019, pp. 16-32.

[9] Zhao, N., Guo, L., Qi, C., Chen, T., and Cui, X, Experimental study on thermo-hydraulic performance of nanofluids in CPU heat sink with rectangular grooves and cylindrical bugles based on exergy efficiency, *Energy Convers. Manag*, Vol. 181, 2019, pp. 235-246.

[10] Sun, B., and Liu, H, Flow and heat transfer characteristics of nanofluids in a liquid-cooled CPU heat radiator, *Appl. Therm. Eng*. Vol. 115, 2017, pp. 435-443.

[11] Snoussi, L., Ouerfelli, N., Sharma, K.V., Vrinceanu, N., Chamkha, A.J., and Guizani, A, Numerical simulation of nanofluids for improved cooling efficiency in a 3D copper microchannel heat sink (MCHS). Physics and Chemistry of Liquids, an International Journal, Vol. 56, No. 3, 2018, pp. 311-331.

[12] Shouka, A. A., Shaban, M., Israr, A., Shah, O. R., Khan, M. Z., and Anwar, M, Stability of Nanofluids and Their use for Thermal Management of a Microprocessor: an Experimental and Numerical Study, *Heat and Mass Transfer*, Vol. 54, 2018, pp. 2771-2782.

[13] Chen, T., Qi, C., Tang, J., Wang, G., and Yan, Y, Numerical and experimental study on optimization of CPU system cooled by nanofluids, *Case Studies in Thermal Engineering*, Vol. 24, 2021, pp. 1-9.

[14] Izadi, M., Sheremet, M. A., Mehryan, S. A. M., Pop, I., Öztop, H. F., and Abu-Hamdeh, N, MHD thermogravitational convection and thermal radiation of a micropolar nanoliquid in a porous chamber, *Int. Commun. Heat Mass Tran*, Vol. 110, 2020, 104409.

[15] Elbadawy, I., and Fayed, M, Reliability of Al_2O_3 nanofluid concentration on the heat transfer augmentation and resizing for single and double stack microchannels, *Alexandria Engineering Journal*, Vol. 59, No. 3, 2020, pp. 1771-1785.

[16] Amiri, E. O., and chali, M. G. A, Numerical Studies of Flow and Temperature Distribution in a Micro-heat Exchanger, *Arabian Journal for Science and Engineering*, Vol. 45, No. 9, 2020, pp. 7667-7675.

[17] Maher, A. R., Al-Baghdadi, S., Noor, Z. M. H., Zeiny, A., Burns, A., and Wen, D, CFD analysis of a nanofluid-based microchannel heat sink, *Thermal Science and Engineering Progress*, Vol. 20, 2020, 100685.

[18] Mohd, W., Japar, A. A., Sidik, N. A. C., Saidur, R., Asako, Y., and Yusof, S. N. A, A review of passive methods in microchannel heat sink application through advanced geometric structure and nanofluids: Current advancements and challenges, *Nanotechnology Reviews*, Vol. 9, No. 1, 2020, pp. 1192-1216.

[19] Mokrane, M., Lounis, M., Announ, M., Ouali, M., Djebiret, M. A., and Bourouis, M, Performance analysis of a micro heat exchanger in electronic cooling applicattions, *Journal of Thermal Engineering*, Vol. 7, No. 4, 2021, pp. 773-790.

[20] Souby, M. M., Bargal, M. H. S., and Wang, Y, Thermohydraulic performance improvement and entropy generation characteristics of a micro channel heat sink cooled with new hybrid nanofluids containing ternary/binary hybrid nanocomposites, *Energy Science & Engineering*, Vol. 9, No. 12, 2021, pp. 2493-2513.

[21] Ramadhan, A. I., Azmi, W. H., and Mamat, R, Stability and Thermal Conductivity of Tri-hybrid Nanofluids for High Concentration in Water-ethylene Glycol (60:40), *Nanoscience & Nanotechnology-Asia*, Vol. 11, No. 4, 2021, pp. 1-11.

[22] Payal, and P. Pandey. Role of Nanotechnology in Electronics: A Review of Recent Developments and Patents. Recent Patents on Nanotechnology, 16 (1) (2022) 45 – 66.

[23] Sanpui, D., Sarkar, S., and Sen, S, Natural Convection of Copper-Water Nanofluid in a Square Enclosure with an Isothermal Protruding Heater. In: Ghosh S.K., Ghosh K., Das S., Dan P.K., Kundu A. (eds) *Advances in Thermal Engineering*, Manufacturing, and Production Management. ICTEMA 2020. Lecture Notes in Mechanical Engineering. Springer, Singapore. 2021.

[24] Mirzaei, R., Ghalambaz, M., and Noghrehabadi, A, Study of the flow and heat transfert of a viscoelastic fluid using hybrid neural network-particle swarm optimization (HNNPSO), *Journal of Thermal Engineering*, Vol. 7, No. 4, 2021, pp. 791-805.

[25] Çakmak, N. K., Durmazuçar, H. H., and Yapicia, K, Numerical study of the natural convection of Al_2O_3-EG nanofluid in a square enclosure and impacts and a comparison of various viscosity and thermal conductivity models, *International Advanced Researches and Engineering Journal*, Vol. 5 No. 5, 2021, pp. 218-230.

[26] Abdulkadhim, A., Abed, I. M. and Said, N. M, An exhaustive review on natural convection within complex enclosures: Influence of various parameters, *Chinese Journal of Physics*, Vol. 74, 2021, pp. 365-388.

[27] Roy, N. C., Yesmin, F., Saha, L. K., and Siddiqa, S, Electrohydrodynamics natural convection flow of nanofluids in a rectangular cavity enclosed by a corrugated bottom surface, *Fluid Dynamics Research*, Vol. 53, No. 1, 2021, 015512.

[28] Taloub, D., Bouras, A., and Driss, Z, Numerical investigation of heat transfer with natural convection in a regularly heated elliptical cylinder submerged in a square fence loaded with a nanofluid, *International journal of mathematical models and methods in applied sciences*, Vol. 15, 2021, pp. 223-232.

[29] Taloub, D., Bouras, A., and Driss, Z, Numerical study of heat transfer by natural convection in concentric hexagonal cylinders charged with a nanofluid, *Wseas transaction on heat and mass transfer*, Vol. 17, 2022, pp. 19-28.

[30] Aminossadati, S. M., Ghasemi, B, Enhanced natural convection in an isosceles triangular enclosure filled with a nanofluid, *Computers and Mathematics with Applications*, Vol. 61, 2011, pp. 1739–1753.

[31] Haq, R. U., Soomro, F. A., Öztop, H. F., and Mekkaoui, T. . Thermal management of water-based carbon nanotubes enclosed in a partially heated triangular cavity with heated cylindrical obstacle, *International Journal of Heat and Mass Transfer*, Vol. 131, No. 5, 2018, pp. 724-736.

[32] Sojoudi, A, Lattice Boltzmann Simulation of Mixed Convection Flow in a Lid-Driven Triangular Cavity Subjected to Sinusoidal Thermal Forcing Utilizing Nanofluid, *American Journal of Fluid Dynamics*, Vol. 8, No. 3, 2018, pp. 84-95.

[33] Mahalakshmi, T., Nithyadevi, N., Oztop, H. F., and Abu-Hamdeh, N, Natural convective heat transfer of Ag-water nanofluid flow inside enclosure with center heater and bottom heat source, *Chinese Journal of Physics*, Vol. 56, No. 4, 2018, pp. 1497-1507.

[34] Oudina, F. M, Convective heat transfer of Titania nanofluids of different base fluids in cylindrical annulus with discrete heat source, *Heat Transfer—Asian Research*, Vol. 48, No. 1, 2019, pp. 135-147.

[35] Loenko, S. D., Shenoy, A., and Sheremet, M. A, Natural Convection of Non-Newtonian Power-Law Fluid in a Square Cavity with a Heat-Generating Element, *Energies*, Vol. 12, No. 1, 2019, pp. 1-12.

[36] Dogonchia, A. S., and Ali, H, Heat transfer by natural convection of Fe_3O_4-water nanofluid in an annulus between a wavy circular cylinder and a rhombus, *International Journal of Heat and Mass Transfer*, Vol. 130, No. 23, 2019, pp. 320-332.

[37] Mebarek-Oudina, F., Keerthi Reddy, N., and Sankar, M, (2021) Heat Source Location Effects on Buoyant Convection of Nanofluids in an Annulus. In: Rushi Kumar B., Sivaraj R., Prakash J. (eds) *Advances in Fluid Dynamics*. Lecture Notes in Mechanical Engineering. Springer, Singapore.

[38] Laidoudi, H, Buoyancy-driven flow in annular space from two circular cylinders in tandem arrangement, *Metall. Mater. Eng*, Vol. 26, No. 1, 2020, pp. 87-102.

[39] Nguyen, T. K., Soomro, F. A., Ali, J. A., Haq, R. U., Sheikholeslami, M., and Shafee, A, Heat transfer of ethylene glycol-nanofluid enclosed by curved porous cavity including electric field, *Physica A: Statistical Mechanics and its Applications*, Vol. 550, No. 15, 2020, 123945.

[40] Umavathi, J. C., and Anwar Bég, O, Modeling the onset of thermosolutal convective instability in a non-Newtonian nanofluid-saturated porous medium layer, *Chinese Journal of Physics*, Vol. 68, 2020, pp. 147-167.

[41] Lakshmi, K. M., Siddheshwar, P. G., and Laroze, D, Natural convection of water-copper nanoliquids confined in low-porosity cylindrical annuli, *Chinese Journal of Physics*, Vol. 68, 2020, pp. 121-136.

[42] Mehryan, S. A. M., Ghalambaz, M., Chamkha, A. J., and Izadi, M, Numerical study on natural convection of Ag–MgO hybrid/water nanofluid inside a porous enclosure: A local thermal non-equilibrium model, *Powder Technology*, Vol. 367, No. 1, 2020, pp. 443-455.

[43] Abdulkadhim, A., Abed, I. M., and Said, N. M, Review of Natural Convection within Various Shapes of Enclosures, *Arab. J. Sci. Eng*, Vol. 46, 2021, pp. 11543–11586.

[44] Alomar, O. R., Mohamed, I. A., Yousif, Q. A., and Abd, H. M, A thermal nonequilibrium model to natural convection inside non-Darcy porous layer surrounded by horizontal heated plates with periodic boundary temperatures, *Heat Transfer*, Vol. 50, No. 6, 2021, pp. 6068-6098.

[45] Alomar, O. R., Basher, N., and Yousif A. A, Natural convection heat transfer from a bank of orthogonal heated plates embedded in a porous medium using LTNE model: A comparison between in-line and staggered arrangements, *International Journal of Thermal Sciences*, Vol. 160, 2021, 106692.

[46] Ali, O. M., and Alomarb, O. R, Mixed convection heat transfer from two aligned horizontal heated cylinders in a vented square enclosure, *Thermal Science and Engineering Progress*, Vol. 25, No. 1, 2021, 101041.

[47] Shariat, M., Akbarinia, A., Hossein Nezhad, A., Behzadmehr, A., and Laur, R, Numerical study of two phase laminar mixed convection nanofluid in elliptic ducts, *Appl. Therm. Eng*, Vol. 31, 2011, pp. 2348-2359.

[48] Izadi, M., Behzadmehr, A., and Jalali-Vahida, D, Numerical study of developing laminar forced convection of a nanofluid in an annulus, *Int. J. Therm. Sci*, Vol. 48, 2009, pp. 2119-2129.

[49] Lotfi, R., Saboohi, Y., and Rashidi, A. M, Numerical study of forced convective heat transfer of nanofluids: comparison of different

approaches, *Int. Commun. Heat Mass Transf*, Vol. 37, 2010, pp. 74-78.

[50] Mokhtari Moghari, R., Akbarinia, A., Shariat, M., Talebi, F., and Laur, R, Two phase mixed convection Al_2O_3 water nanofluidflow in an annulus, *Int. J. Multiph. Flow*, Vol. 37, 2011, pp. 585-595.

[51] Nuim Labib, M., Nine, Md. J., Afrianto, H., Chung, H., and Jeong, H, Numerical investigation on effect of basefluids and hybrid nanofluid in forced convective heat transfer, *Int. J. Therm. Sci*, Vol. 71, 2013, pp. 163-171.

[52] Kim, C. S., Okuyama, K., and Fernandez, J. De La Mora, Performance evaluation of an improved particle size magnifier (PSM) for single nanoparticle detection, *Aerosol Science and Technology*, Vol. 37, No. 10, 2003, pp. 791–803.

[53] Abu-Nada, E., Masoud, Z., and Hijazi, A, Natural convection heat transfer enhancement in horizontal concentric annuli using nanofluids, *International Communications in Heat and Mass Transfer*, Vol. 35, No. 5, 2008, pp. 657–665.

[54] Khentoul, M. and Bessaïh, R, Numerical Simulation of Nanofluid Cooling Enhancement of Three Fins Mounted in a Horizontal Channel, *Journal of Heat Transfer*, Vol. 138, 2016, 091002.

[55] Maxwell, J. C., A Treatise on Electricity and Magnetism, vol. II, Oxford University Press, Cambridge, UK, 1873, pp. 54.

[56] Patankar, S., Spalding, D, A calculation procedure for heat, mass and momentum transfer in three-dimensional parabolic flows. Int. J. heat and Mass transfer, vol. 15, pp. 1787-1806, 1972.